Calorimetric measurements of structural relaxation and glass transition temperatures in sputtered films of amorphous Te alloys used for phase change recording

J.A. Kalb[a)]
I. Physikalisches Institut der Rheinisch-Westfälischen Technischen Hochschule (RWTH) Aachen, 52056 Aachen, Germany; Division of Engineering and Applied Sciences, Harvard University, Cambridge, Massachusetts 02138; and Department of Materials Science and Engineering, Massachusetts Institute of Technology, Cambridge, Massachusetts 02139

M. Wuttig
I. Physikalisches Institut der Rheinisch-Westfälischen Technischen Hochschule (RWTH) Aachen, 52056 Aachen, Germany

F. Spaepen[b)]
Division of Engineering and Applied Sciences, Harvard University, Cambridge, Massachusetts 02138

(Received 16 September 2006; accepted 24 November 2006)

Sputtered amorphous $Ge_4Sb_1Te_5$, $Ge_1Sb_2Te_4$, $Ge_2Sb_2Te_5$, and $Ag_{0.055}In_{0.065}Sb_{0.59}Te_{0.29}$ thin films were studied by differential scanning calorimetry. Upon continuous heating, heat release due to structural relaxation of the amorphous phase between 0.5 and 1.0 kJ/mol was observed. This value depends on the thermal history of the sample. Preannealing of the amorphous phase revealed the glass transition temperature T_g within 10 K of the crystallization temperature upon continuous heating at 40 K/min.

I. INTRODUCTION

Tellurium alloys are used for optical data storage in commercial rewritable phase change media. In rewritable compact disks (CDs) and digital video disks (DVDs), a thin film of a Te alloy is locally and reversibly switched by laser heating between the amorphous and crystalline states. These states can be distinguished optically by their difference in reflectivity.[1] Due to the reversibility of the transition on the nanosecond timescale, the term "phase change materials" is widely used for those alloys. Recently, phase change materials have also shown high potential for future electronic non-volatile data storage.[2] In these so-called "phase change random access memories" (PC-RAMs), electrical power provides the heat that is necessary for transformations between the amorphous and crystalline states, which can be distinguished subsequently by their pronounced difference in electrical conductivity.[2–5]

To develop programmable resistor elements on the nanometer scale for the next generation of phase change media, it is mandatory to understand the crystallization kinetics of phase change materials in more detail. Those can be separated into the two contributions of nucleation and growth.[6,7] Both the crystal nucleation rate and the crystal growth velocity are inversely proportional to the shear viscosity η in the undercooled liquid state.[6–12] Unfortunately, little is known about η and its temperature dependence for phase change materials because the undercooled liquid state is not easily available for experiments due to rapid crystallization. Due to this uncertainty, it has usually been difficult to model the crystal nucleation rate and the crystal growth velocity with satisfactory accuracy.[13–16] Close to the glass transition temperature T_g, at which the viscosity of the undercooled liquid is on the order of 10^{12} Pa s,[17–19] the crystal nucleation rate and the crystal growth velocity are dominated by the viscosity. This is because the viscosity increases rapidly around T_g upon cooling, which causes the crystal nucleation rate and the crystal growth velocity to become negligibly small. This strongly affects the overall shape of the nucleation rate and growth velocity curves as a function of temperature. Hence, the knowledge of the glass transition temperature significantly helps to model and understand crystallization kinetics.

No unambiguous experimental evidence for the glass transition in phase change materials has been found so far. Speculations, however, are numerous. Mansuripur and co-workers[13] assumed a value of $T_g = 400$ °C to model crystallization and amorphization kinetics of $Ge_2Sb_2Te_5$. Hudgens and Johnson[2] assumed $T_g = 350$ °C for the same alloy. Lankhorst[20] presented a model for estimating T_g for a variety of phase change materials based on the enthalpy of atomization. He obtained values

[a)]Address all correspondence to this author.
e-mail: art.tg@kalb.eu
[b)]This author was Chair of the *JMR* Advisory Review Board during the review and decision stage.
DOI: 10.1557/JMR.2007.0103

for T_g that are in many cases much lower than the crystallization temperature[3–5,21–24] upon heating at low and moderate rates ($\dot{T} < 100$ K/min), e.g., $T_g = 190$ °C ($Ge_4Sb_1Te_5$), $T_g = 77$ °C ($Ge_1Sb_2Te_4$), $T_g = 111$ °C ($Ge_2Sb_2Te_5$), and $T_g \sim 80$ °C (AgIn-doped Sb_2Te). Morales-Sanchez and co-workers[25] reported experimental evidence for the glass transition of $Ge_2Sb_2Te_5$ around 100 °C by differential scanning calorimetry (DSC). However, the data presented in Ref. 25 are limited and difficult to interpret. Finally, the authors of the present article have assumed[21] the glass transition temperatures of $Ge_4Sb_1Te_5$, $Ge_2Sb_2Te_5$, and $Ag_{0.055}In_{0.065}Sb_{0.59}Te_{0.29}$ to be close to the crystallization temperature of the amorphous phase upon furnace heating, i.e., between around 150 and 200 °C depending on the alloy. Using this assumption, they made quantitative predictions of the crystal nucleation rate in the undercooled liquid as a function of temperature.[26] In this article, we present unambiguous experimental evidence of the glass transition by DSC measurements for the phase change materials mentioned above.

II. EXPERIMENTAL TECHNIQUES

A solution of 3 vol% polymethyl methacrylate (PMMA) dissolved in chlorobenzene was deposited by spin coating (4000 revolutions per minute) on glass microscope slides. Films of composition $Ge_1Sb_2Te_4$, $Ge_2Sb_2Te_5$ (the material of choice in DVD-RAM), and $Ag_{0.055}In_{0.065}Sb_{0.59}Te_{0.29}$ (similar in composition to the material of choice in DVD+RW and DVD-RW, hereafter AgIn–Sb_2Te) were deposited on those PMMA layers by dynamic direct current magnetron sputtering from a single commercial target. Films of composition $Ge_4Sb_1Te_5$ were deposited on thin plates of stainless steel by static direct current magnetron sputtering from a single commercial target. For all depositions, the background pressure was approximately 10^{-6} mbar, and the working pressure during sputtering in Ar ambient was 7×10^{-3} mbar. The sputtering powers were 50 W ($Ge_1Sb_2Te_4$), 25 W ($Ge_2Sb_2Te_5$ and AgIn–Sb_2Te), and 100 W ($Ge_4Sb_1Te_5$). The deposition rates were approximately 0.25 nm/s ($Ge_1Sb_2Te_4$, $Ge_2Sb_2Te_5$, and AgIn–Sb_2Te) and 2 nm/s ($Ge_4Sb_1Te_5$). The target diameters were 5 cm ($Ge_2Sb_2Te_5$ and AgIn–Sb_2Te) and 10 cm ($Ge_1Sb_2Te_4$ and $Ge_4Sb_1Te_5$). The target–substrate distance was 5 cm in all cases. The film thicknesses were 1500 nm ($Ge_1Sb_2Te_4$, $Ge_2Sb_2Te_5$, and AgIn–Sb_2Te), and 7000 nm ($Ge_4Sb_1Te_5$). The film compositions were confirmed previously by inductively coupled plasma emission spectroscopy, energy dispersive x-ray spectroscopy, and Rutherford backscattering.[5,21,24,27,28] After deposition, the PMMA layer underneath the $Ge_1Sb_2Te_4$, $Ge_2Sb_2Te_5$, and AgIn–Sb_2Te films was dissolved in acetone. For $Ge_4Sb_1Te_5$, the substrate was bent so the films could be peeled off. Both methods gave sample fragments on the order of a few square millimeters. X-ray diffraction (XRD) showed that the structure of the as-deposited films was amorphous. The samples were prepared without capping layers.

A power-compensated DSC (Perkin Elmer Pyris1/Diamond, Wellesley, MA), calibrated with the melting point and enthalpy of fusion of indium and zinc, was used to measure the heat flow, $\dot{H} = dH/dt$ (H is enthalpy), into the sample. About 5–10 mg film fragments were sealed in standard aluminum pans and scanned at constant heating and cooling rates. The atmosphere was high-purity argon. In contrast to our previous study by DSC,[21] special attention was paid to the measurement of the baselines to observe and measure structural relaxation curves.

III. RESULTS AND DISCUSSION

Figure 1 displays the heat flow as a function of temperature T for all as-prepared alloys. A scan rate of $\dot{T} = \pm 40$ K/min turned out to be most useful to reveal the thermal signals. From earlier XRD measurements, the large exothermic peak upon heating of the initially amorphous sample (lower solid curve in Fig. 1, labeled "first scan") can be identified with crystallization.[3–5,22,23,29] The coordinates of the peak position, $T_{c,p}$ and $\dot{H}_p$, and the heat of crystallization ΔH_c are given in Table I. For $Ge_4Sb_1Te_5$ and AgIn–Sb_2Te, the values for ΔH_c in Table I agree with the values reported in our earlier study.[21] For $Ge_2Sb_2Te_5$, ΔH_c in Table I is higher than our earlier value, which was only an estimate due to overlapping signals, baseline reproducibility problems, and strong baseline curvature.[21] In the present study, these problems have been solved by using thoroughly polished DSC furnaces. This resulted in a significantly improved similarity between the two furnaces, which enabled us to minimize baseline curvature. Yamada and co-workers[23] obtained a value of $\Delta H_c = 3.1$ kJ/mol for $Ge_1Sb_2Te_4$, which coincides with the value obtained in this work (Table I).

The upper solid curve in Fig. 1 is the rescan of the crystallized sample. It does not reveal thermal transformations and was reproduced in several additional heating cycles as long as sample and reference remained at the same positions in the DSC furnaces. Hence, the rescan serves as a baseline for the first scan (lower curve). A comparison of these two curves shows a heat release to the left side of the main crystallization peak, starting at a temperature T_1. This cannot be ascribed to crystallization because the isothermal time lag τ for nucleation at the temperature T_1 (defined as the time at which the first crystal nucleates) is too long to allow crystallization.[30] Furthermore, the isothermal crystal growth velocity u is far too slow at T_1 to observe crystallization.[31] For example, our earlier measurements of crystallization

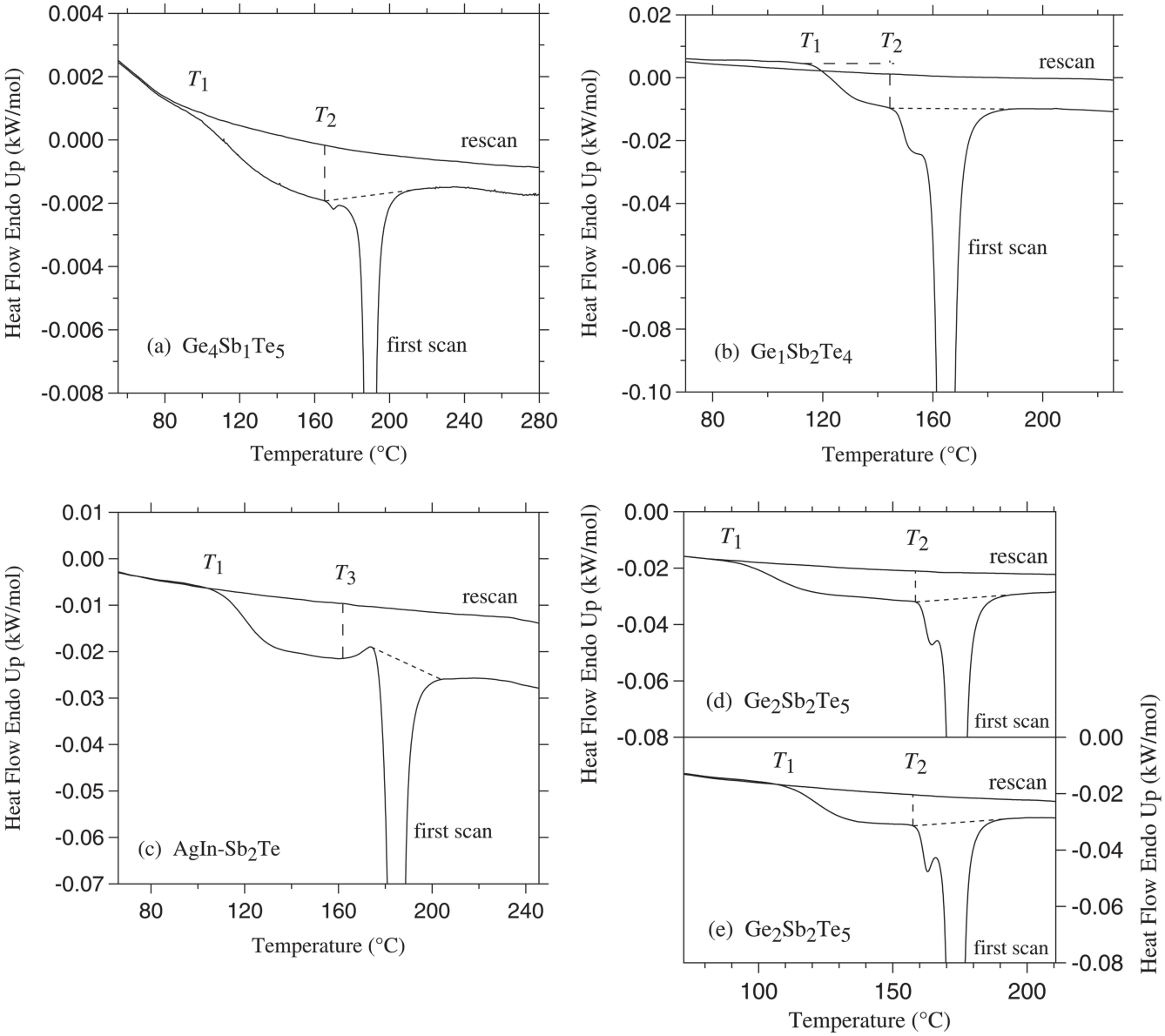

FIG. 1. Heat flow as a function of temperature: (a) $Ge_4Sb_1Te_5$, sample age: 27 days; (b) $Ge_1Sb_2Te_4$, sample age: 106 days; (c) AgIn–Sb_2Te, sample age: 33 days; (d) $Ge_2Sb_2Te_5$, sample age: 3 days; and (e) $Ge_2Sb_2Te_5$, sample age: 39 days. Lower solid curve: first scan for the initially fully amorphous sample (heating). Due to its large extension, the main (exothermic) crystallization peak is not entirely shown for all alloys to make the baseline more visible. The quantities associated with the main crystallization peak are shown in Table I. Upper solid curve: rescan of the crystallized sample (heating, reproduced in additional scans). The scan rate was $\dot{T} = 40$ K/min for all alloys, except for $Ge_4Sb_1Te_5$, where it was $\dot{T} = 5$ K/min. Comparison of the first scan and the rescan (the latter serves as a baseline) reveals the onset of observable structural relaxation at T_1, the onset of surface crystallization at T_2, and the onset of the endothermic signal characteristic of the glass transition at T_3.

parameters by atomic force microscopy (AFM)[30,31] showed that $\tau(140\ °C) \sim 50$ min and $u(140\ °C) \sim 8$ Å/min for AgIn–Sb_2Te, and $\tau(115\ °C) \sim 4$ h and $u(115\ °C) \sim 4$ Å/min for $Ge_2Sb_2Te_5$. The exothermic heat flow at T_1 can be ascribed to structural relaxation of the amorphous phase, which is usually accompanied by heat release (dotted curve in Fig. 2).[17,32–34] As shown in Figs. 1(d) and 1(e), the onset temperature T_1 for observable structural relaxation increases with increasing sample age (the time the sample was stored at room temperature before the experiment). The heat release during structural relaxation ΔH_{str} was obtained from the area to the left of the vertical dashed line in Fig. 1 (integral from T_1 to T_2 for the GeSbTe alloys and from T_1 to T_3 for AgIn–Sb_2Te) and is given in Table I. The comparison of Figs. 1(d) and 1(e) shows that sample age affects ΔH_{str}. For this reason, a "quantitative" comparison of ΔH_{str} and T_1 between different alloys is not possible since their aging times at room temperature have been different (see caption of Fig. 1). The main point of Fig. 1 is to show "qualitatively" that structural relaxation is present in all alloys. A broad, exothermic signal from structural relaxation has

TABLE I. Peak coordinates $T_{c,p}$ and $\dot{H}_p$ of the main crystallization peak (not entirely shown in Figs. 1 and 3 for better baseline visibility) during the first scan of the initially amorphous sample.

Figure	Alloy	$T_{c,p}$[a] (°C)	$\dot{H}_p$[b] (kW/mol)	ΔH_{str}[c] (kJ/mol)[e]	ΔH_c[d] (kJ/mol)[e]
1(a)	$Ge_4Sb_1Te_5$	190.2	–0.126	0.99 ± 0.05	3.9 ± 0.1
1(b)	$Ge_1Sb_2Te_4$	164.6	–0.398	0.34 ± 0.05	3.1 ± 0.1
1(c)	AgIn-Sb_2Te	184.3	–0.987	0.72 ± 0.05	4.3 ± 0.1
1(d)	$Ge_2Sb_2Te_5$	173.4	–0.776	0.80 ± 0.05	3.9 ± 0.1
1(e)	$Ge_2Sb_2Te_5$	172.9	–0.900	0.58 ± 0.05	3.9 ± 0.1
3(a)	$Ge_4Sb_1Te_5$	215.9	–0.664	⋯	⋯
3(b)	$Ge_1Sb_2Te_4$	168.1	–0.478	⋯	⋯
3(c)	AgIn-Sb_2Te	184.3	–1.249	⋯	⋯
3(d)	$Ge_2Sb_2Te_5$	183.3	–1.002	⋯	⋯

[a]$T_{c,p}$ is the peak crystallization temperature.
[b]$\dot{H}_p$ is the peak heat flow signal. The heating rate was $\dot{T} = 40$ K/min for all scans, except for the scan shown in Fig. 1(a), where it was $\dot{T} = 5$ K/min. For this reason, the peak height in Fig. 1(a) is lower.
[c]ΔH_{str} is the heat that is released in the amorphous phase during structural relaxation (integral of the thermal curve in Fig. 1 from T_1 to T_2 for the GeSbTe alloys and from T_1 to T_3 for AgIn-Sb_2Te; i.e., the area to the left of the vertical dashed line in Fig. 1).
[d]ΔH_c is the heat of crystallization (determined by the area underneath the dotted line in Fig. 1). ΔH_c in Fig. 3 is the same as in Fig. 1 (for the same alloy) but is not listed here.
[e]1 kJ/mon = $1000/(eN_A)$ eV/atom ≈ 10.4 meV/atom. *e:* elementary charge; N_A: Avogadro's number.

also been observed in many other amorphous materials and is attributed to the presence of a spectrum of activation energies for the sites where relaxation occurs.[32,35–37] Prolonged isothermal annealing, for example at room temperature, eliminates the sites with the lowest activation energies. As a result, upon heating a lower heat of relaxation ΔH_{str} and a higher onset T_1 are observed.

At the temperature T_2, an onset to a small exothermic peak occurs for the GeSbTe alloys (this peak is less pronounced for $Ge_4Sb_1Te_5$). This can be ascribed to heterogeneous nucleation at the (naturally oxidized) sample surface. It is known from cross-sectional transmission electron microscopy that the sample surface of naturally oxidized GeSbTe alloys crystallizes prior to the rest of the film.[30,38] Surface crystallization effects similar to those shown in Fig. 1 have also been observed in 4-point-probe electrical film resistance measurements[39] and stress measurements[40] upon heating naturally oxidized GeSbTe alloys of the same composition as those studied here. For AgIn–Sb_2Te [Fig. 1(c)], no indication for surface crystallization is observable. It is possible that this alloy oxidizes significantly more slowly than the GeSbTe alloys due to the lack of Ge. This suggests that the predominate oxide at the surface of the GeSbTe alloys is GeO_2.

Crystallization of $Ge_1Sb_2Te_4$ and $Ge_2Sb_2Te_5$ has been studied intensely by DSC over the past 20 years, but all of those studies have focused on the determination of the peak crystallization temperature $T_{c,p}$.[21–23,29,38,41–43]

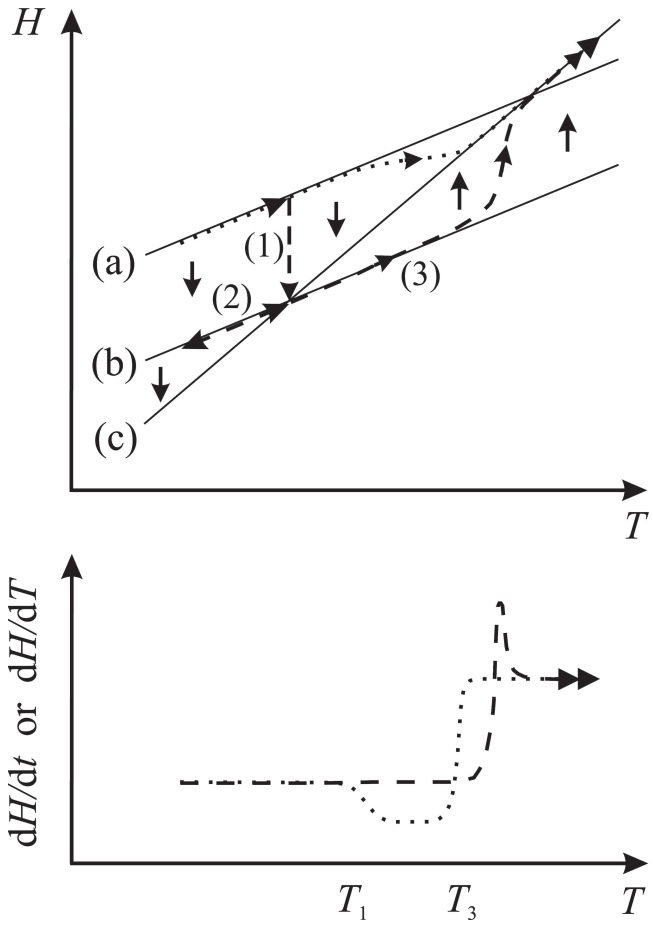

FIG. 2. (Top graph) Schematic evolution of the enthalpy H as a function of temperature T. The solid lines (a) and (b) denote isoconfigurational states (amorphous phase). The undercooled liquid (equilibrium) is denoted by solid line (c). Structural relaxation of the amorphous phase changes the enthalpy of the amorphous phase toward the enthalpy of the undercooled liquid (short solid arrows). Dotted curve: Enthalpy evolution during continuous heating without pre-annealing (corresponds to Fig. 1). Dashed curve: Enthalpy evolution during (1) pre-annealing, (2) cooling, and (3) subsequent continuous heating at the "same" rate as for the dotted curve (corresponds to Fig. 3). (Bottom graph) Time or temperature derivative of the enthalpy H as measured in the DSC. The dashed (dotted) curve in the lower graph corresponds to the dashed (dotted) curve in the upper graph. Endothermic signals are positive. The onset of structural relaxation at T_1 is accompanied by an exothermic signal. T_1 depends on thermal history: the more relaxed the amorphous phase is, the higher T_1 [Figs. 1(d) and 1(e)]. If the pre-anneal is long enough (vertical dashed arrow labeled 1 in the top graph), the exothermic heat release at T_1 is not observed during subsequent heating. The onset of the endothermic signal characteristic of the glass transition at T_3 is more pronounced if the sample is pre-annealed (dashed curve in the bottom graph).

Even though in some studies of $Ge_1Sb_2Te_4$ and $Ge_2Sb_2Te_5$ a heat release is visible in the amorphous phase,[29,41,42] this effect has neither been related to structural relaxation nor surface crystallization, mostly because no reference was made to a reproducible baseline. Our earlier study[21] revealed indication of such a heat

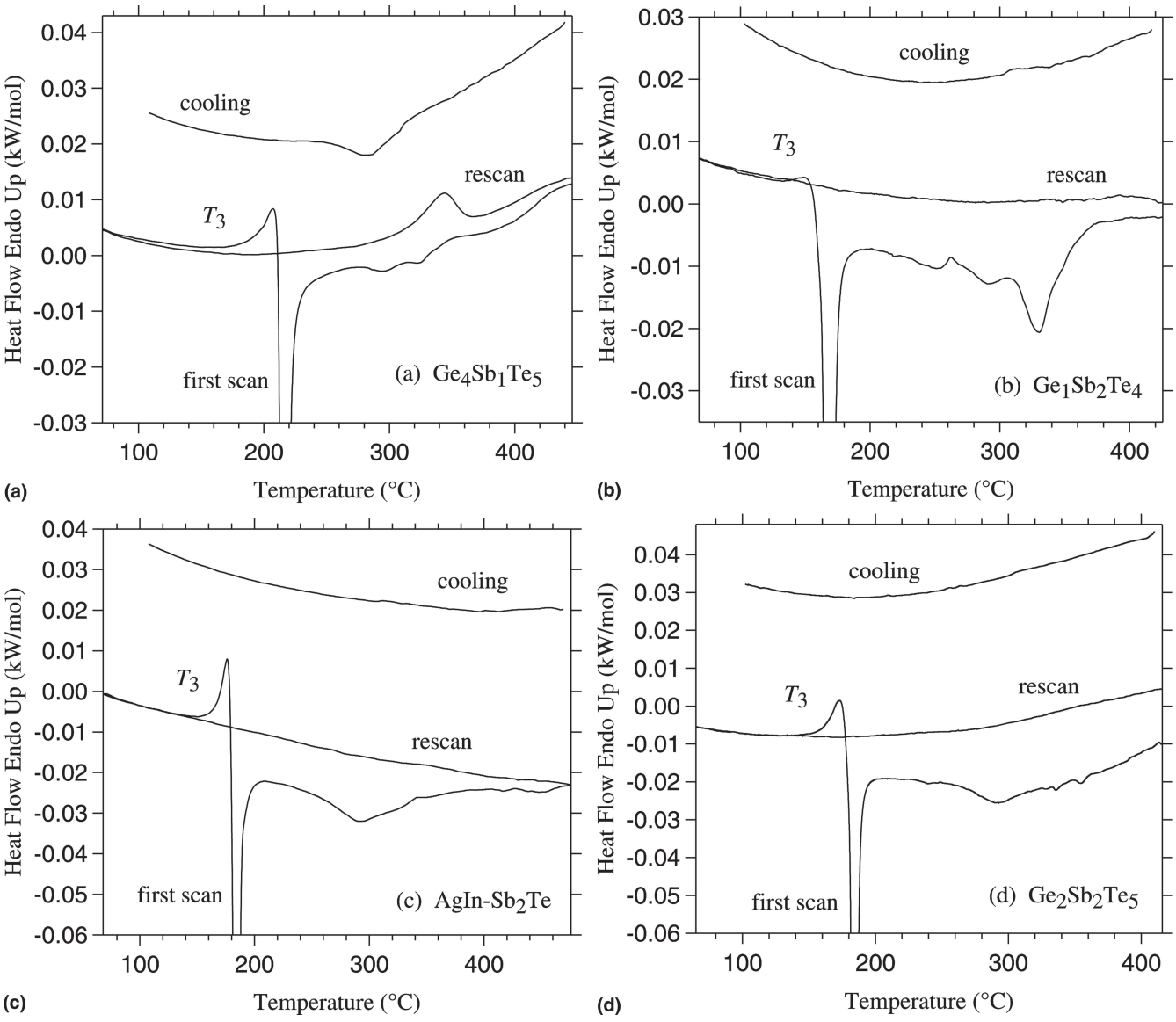

FIG. 3. Heat flow as a function of temperature on pre-annealed samples: (a) $Ge_4Sb_1Te_5$, pre-anneal for 47 h at 136 °C; (b) $Ge_1Sb_2Te_4$, pre-anneal for 40 h at 100 °C; (c) AgIn–Sb_2Te, pre-anneal for 48 h at 112 °C; and (d) $Ge_2Sb_2Te_5$, pre-anneal for 37 h at 114 °C. Lowest curve: first scan for the initially amorphous sample (heating). Due to its large extension, the main (exothermic) crystallization peak is not entirely shown for all alloys to make the baseline more visible. The quantities associated with the main crystallization peak are shown in Table I. The rescan of the crystallized sample (heating) was reproduced in additional scans. Top curve: cooling signal (reproduced in additional scans). For clarity, an arbitrary offset has been added to the cooling signal. The scan rate was $\dot{T} = \pm 40$ K/min for all alloys. The onset of the endothermic signal characteristic of the glass transition occurs at a temperature T_3.

release for $Ge_2Sb_2Te_5$ at around 100 °C as well, but baseline reproducibility problems and strong baseline curvature hampered the precise interpretation of this effect.

The calorimetric signal of the glass transition is an endothermic step since the heat capacity increases due to the availability of configurational degrees of freedom.[17,33,34] In Fig. 1, onset for such a step is visible only for AgIn–Sb_2Te at a temperature T_3. For the other alloys, crystallization interferes, as is common in many other glasses. Because the glass transition is a kinetic phenomenon, it is sometimes possible to reveal T_g by pre-annealing the amorphous phase.[33,34] This is schematically shown in Fig. 2: During the pre-anneal, equilibrium [curve (c)] is approached by structural relaxation (vertical long dashed arrow). This increases the shear viscosity[18,19]; i.e., the viscosity in the isoconfigurational state (b) is higher than in state (a). During subsequent continuous heating (dashed curve in Fig. 2), structural relaxation is initially not observed due to the large viscosity (or equivalently, low atomic mobility). This is in contrast to a sample that was not pre-annealed (dotted curve, Fig. 2), for which structural relaxation is observed

at T_1 for the same heating rate. During further heating of the pre-annealed sample (dashed curve in Fig. 2), the mobility increases and structural relaxation becomes finally very pronounced, leading to a strong endothermic signal in the DSC associated with the glass transition (dashed curve, bottom of Fig. 2). Figure 3 shows the scans on pre-annealed samples. The film fragments were pre-annealed in the DSC under the same condition as for the subsequent heating scan. Pre-anneal time and temperature were chosen in such a way that the surface crystallization was complete. Isothermal surface crystallization parameters (crystal nucleation rate and crystal growth velocity) determined by AFM[30,31] were used for the calculation of the appropriate pre-anneal time and temperature. Hence, no surface crystallization signal appears in Fig. 3 at a temperature T_2. This additionally facilitates the detection of the glass transition, the onset of which appears at a temperature T_3. However, the main crystallization peak interferes so that the endothermic step associated with the glass transition (Fig. 2) cannot be resolved entirely. The peak crystallization temperature $T_{c,p}$ of the pre-annealed samples increases by a few Kelvin (Table I) due to a higher viscosity in the amorphous phase prior to crystallization. For AgIn–Sb_2Te, $T_{c,p}$ was not affected by the pre-anneal. The reason for this behavior remains unclear.

Because the alloy $Ge_4Sb_1Te_5$ was scanned both with a heating rate of 5 K/min [Fig. 1(a)] and 40 K/min [Fig. 3(a)], the reader may be tempted to use the variation in $T_{c,p}$ as a function of heating rate for a Kissinger analysis to reveal the total activation energy for crystallization.[44] However, such a procedure is not appropriate for our data due to the increase in $T_{c,p}$ for pre-annealed samples. A systematic investigation of a series of samples with the same thermal history but different heating rates would be required for this analysis. This is outside the scope of this work.

Figure 3 also reveals heat release in the crystalline phase during the first heating scan (lowest curve). Comparison of this curve with the rescan reveals that this heat release is irreversible. Possible explanations are crystal-to-crystal transformations, phase separation, and grain growth. Indeed, an irreversible crystal-to-crystal-transformation between a cubic and a rhombohedral phase was reported by XRD for $Ge_1Sb_2Te_4$ and $Ge_2Sb_2Te_5$ around 200–300 °C.[4,22,23,29] On the other hand, a separation of an $AgSbTe_2$ phase was reported[45] upon annealing the alloy $Ag_{0.08}In_{0.13}Sb_{0.49}Te_{0.30}$ (similar in composition to our AgIn–Sb_2Te) for 1 h at 350 °C.

$Ge_4Sb_1Te_5$ exhibits a reversible transformation of 0.27 ± 0.04 kJ/mol between 300 and 350 °C (Fig. 3). However, this transformation is not visible in the first scan. Hence, it is likely that phase separation during the first heating scan creates a high-temperatures phase, which transforms reversibly upon subsequent cooling and heating. For the other alloys, the cooling curves do not show any transformations (top curves in Fig. 3).

IV. CONCLUSIONS

The endothermic signal of the glass transition temperature T_g could be observed in the DSC for all phase change alloys studied in this work by pre-annealing the amorphous phase. T_g is within 10 K of the crystallization temperature upon continuous heating at 40 K/min. The presence of the glass transition in this temperature range is corroborated further by the observation of structural relaxation upon continuous heating of the amorphous phase, since structural relaxation is usually most pronounced in the vicinity of the glass transition. The heat released during structural relaxation is on the order of 0.5–1.0 kJ/mol and depends on thermal history.

Knowledge of the glass transition temperature is very helpful to estimate the temperature dependence of the viscosity. Because the crystal nucleation rate and crystal growth velocity crucially depend on this temperature dependence, more reliable calculations of crystallization parameters should now be possible based on the results of this article.

ACKNOWLEDGMENTS

One of the authors (J.A. Kalb) acknowledges the Studienstiftung des Deutschen Volkes for financial support. J.A. Kalb and F. Spaepen acknowledge partial support from the Alexander-von-Humboldt-Stiftung. We thank J. Tomforde for helpful discussions on the sample preparation, H. Dieker for sputtering the samples, and M. Salinga for a careful reading of the manuscript. Work at Harvard is supported in part by the MRSEC program of the National Science Foundation. Financial support by the 6th Framework Program of the European Commission within the CAMELS-Project (Contract No. IST-3-017406) is gratefully acknowledged.

REFERENCES

1. N. Yamada: Erasable phase-change optical materials. *MRS Bull.* **21**(9), 48 (1996).
2. S. Hudgens and B. Johnson: Overview of phase-change chalcogenide nonvolatile memory technology. *MRS Bull.* **29**(11), 829 (2004).
3. D. Wamwangi, W.K. Njoroge, and M. Wuttig: Crystallization kinetics of $Ge_4Sb_1Te_5$ films. *Thin Solid Films* **408,** 310 (2002).
4. I. Friedrich, V. Weidenhof, W. Njoroge, P. Franz, and M. Wuttig: Structural transformations of $Ge_2Sb_2Te_5$ films studied by electrical resistance measurements. *J. Appl. Phys.* **87,** 4130 (2000).
5. W.K. Njoroge and M. Wuttig: Crystallization kinetics of sputter-deposited amorphous AgInSbTe films. *J. Appl. Phys.* **90,** 3816 (2001).
6. J.W. Christian: *The Theory of Transformations in Metals and*

Alloys, 2nd ed. (Pergamon, North-Holland, Amsterdam, The Netherlands, 1975).
7. D.M. Herlach: Non-equilibrium solidification of undercooled metallic melts. *Mater. Sci. Eng., R* **12,** 177 (1994).
8. D. Turnbull: Phase changes. *Solid State Phys.* **3,** 225 (1956).
9. D. Turnbull: Under what conditions can a glass be formed? *Contemp. Phys.* **10,** 473 (1969).
10. C.V. Thompson, A.L. Greer, and F. Spaepen: Crystal nucleation in amorphous $(Au_{100-y}Cu_y)_{77}Si_9Ge_{14}$ alloys. *Acta Metall.* **31,** 1883 (1983).
11. C.V. Thompson and F. Spaepen: Homogeneous crystal nucleation in binary metallic melts. *Acta Metall.* **31,** 2021 (1983).
12. K.F. Kelton: Crystal nucleation in liquids and glasses. *Solid State Phys.* **45,** 75 (1991).
13. C. Peng, L. Cheng, and M. Mansuripur: Experimental and theoretical investigations of laser-induced crystallization and amorphization in phase-change optical-recording media. *J. Appl. Phys.* **82,** 4183 (1997).
14. A.C. Sheila and T.E. Schlesinger: Modeling thermal cross talk and overwrite jitter in growth dominant phase change optical-recording media at high data rates. *J. Appl. Phys.* **91,** 2803 (2002).
15. R. Meinders, H.J. Borg, M.H.R. Lankhorst, J. Hellmig, and A.V. Mijritskii: Numerical simulation of mark formation in dual-stack phase-change recording. *J. Appl. Phys.* **91,** 9794 (2002).
16. S. Senkader and C.D. Wright: Models for phase-change of $Ge_2Sb_2Te_5$ in optical and electrical memory devices. *J. Appl. Phys.* **95,** 504 (2004).
17. S.R. Elliott: *Physics of Amorphous Materials* (Longman, London, UK, 1984).
18. F. Spaepen: *Physics of Defect*s, Les Houches Lectures XXXV, edited by R. Balian, M. Kleman, and J-P. Poirier (North–Holland, Amsterdam, The Netherlands, 1981), p. 133.
19. F. Spaepen and D. Turnbull: Metallic glasses. *Annu. Rev. Phys. Chem.* **35,** 241 (1984).
20. M.H.R. Lankhorst: Modelling glass transition temperatures of chalcogenide glasses. Applied to phase-change optical recording materials. *J. Non-Cryst. Solids* **297,** 210 (2002).
21. J. Kalb, F. Spaepen, and M. Wuttig: Calorimetric measurements of phase transformations in thin films of amorphous Te alloys used for optical data storage. *J. Appl. Phys.* **93,** 2389 (2003).
22. N. Yamada, E. Ohno, N. Akahira, K. Nishiuchi, K. Nagata, and M. Takao: High speed overwritable phase change optical disk material. *Jpn. J. Appl. Phys.* **Suppl. 26-4,** 61 (1987).
23. N. Yamada, E. Ohno, K. Nishiuchi, N. Akahira, and M. Takao: Rapid phase transitions of GeTe–Sb_2Te_3 pseudobinary amorphous thin films for an optical disk memory. *J. Appl. Phys.* **69,** 2849 (1991).
24. T.P. Leervad Pedersen, J. Kalb, W.K. Njoroge, D. Wamwangi, M. Wuttig, and F. Spaepen: Mechanical stresses upon crystallization in phase change materials. *Appl. Phys. Lett.* **79,** 3597 (2001).
25. E. Morales-Sanchez, E.F. Prokhorov, A. Mendoza-Galvan, and J. Gonzalez-Hernandez: Determination of the glass transition and nucleation temperatures in $Ge_2Sb_2Te_5$ sputtered films. *J. Appl. Phys.* **91,** 697 (2002).
26. J.A. Kalb, F. Spaepen, and M. Wuttig: Kinetics of crystal nucleation in undercooled droplets of Sb- and Te-based alloys used for phase change recording. *J. Appl. Phys.* **98,** 054910 (2005).
27. I. Friedrich, V. Weidenhof, S. Lenk, and M. Wuttig: Morphology and structure of laser-modified $Ge_2Sb_2Te_5$ films studied by transmission electron microscopy. *Thin Solid Films* **389,** 239 (2001).
28. J. Kalb, F. Spaepen, T.P. Leervad Pedersen, and M. Wuttig: Viscosity and elastic constants of thin films of amorphous Te alloys used for optical data storage. *J. Appl. Phys.* **94,** 4908 (2003).
29. F.X. Gan, S.S. Xue, and Z.X. Fan: Metastable phase formation and structural change characteristics of vapor deposited semiconductor films. *Ann. Phys.* **1,** 391 (1992).
30. J.A. Kalb, C.Y. Wen, F. Spaepen, H. Dieker, and M. Wuttig: Crystal morphology and nucleation in thin films of amorphous Te alloys used for phase change recording. *J. Appl. Phys.* **98,** 054902 (2005).
31. J. Kalb, F. Spaepen, and M. Wuttig: Atomic force microscopy measurements of crystal nucleation and growth rates in thin films of amorphous Te alloys. *Appl. Phys. Lett.* **84,** 5240 (2004).
32. T-W. Wu and F. Spaepen: The relation between enbrittlement and structural relaxation in an amorphous metal. *Philos. Mag. B* **61,** 739 (1990).
33. C.T. Moynihan, P.B. Macedo, C.J. Montrose, P.K. Gupta, M.A. DeBolt, J.F. Dill, B.E. Dom, P.W. Drake, A.J. Easteal, P.B. Elterman, R.P. Moeller, H. Sasabe, and J.A. Wilder: Structural relaxation in vitreous materials. *Ann. N. Y. Acad. Sci.* **279,** 15 (1976).
34. R.B. Stephens: The viscosity and structural relaxation rate of evaporated amorphous selenium. *J. Appl. Phys.* **49,** 5855 (1978).
35. S. Roorda, S. Doorn, W.C. Sinke, P.M.L.O. Scholte, and E. van Loenen: Calorimetric evidence for structural relaxation in amorphous silicon. *Phys. Rev. Lett.* **62,** 1880 (1989).
36. E.P. Donovan, F. Spaepen, D. Turnbull, J.M. Poate, and D.C. Jacobson: Calorimetric studies of crystallization and relaxation of amorphous Si and Ge prepared by ion implantation. *J. Appl. Phys.* **57,** 1795 (1985).
37. E.P. Donovan, F. Spaepen, J.M. Poate, and D.C. Jacobson: Homogeneous and interfacial heat releases in amorphous silicon. *Appl. Phys. Lett.* **55,** 1516 (1989).
38. T.H. Jeong, M.R. Kim, H. Seo, S.J. Kim, and S.Y. Kim: Crystallization behavior of sputter-deposited amorphous $Ge_2Sb_2Te_5$ thin films. *J. Appl. Phys.* **86,** 774 (1999).
39. W.K. Njoroge: Phase change optical recording–preparation and x-ray characterization of GeSbTe and AgInSbTe films. Ph.D. Thesis, Rheinisch-Westfälische Technische Hochschule (RWTH), Aachen, Germany (2001).
40. T.P. Leervad Pedersen: Mechanical stresses upon phase transitions. Ph.D. Thesis, Rheinisch-Westfälische Technische Hochschule (RWTH), Aachen, Germany (2003).
41. H. Seo, T-H. Jeong, J-W. Park, C. Yeon, S-J. Kim, and S-Y. Kim: Investigation of crystallization behavior of sputter-deposited nitrogen-doped amorphous $Ge_2Sb_2Te_5$ thin films. *Jpn. J. Appl. Phys.* **39,** 745 (2000).
42. D. Chiang, T-R. Jeng, D-R. Huang, Y-Y. Chang, and C-P. Liu: Kinetic crystallization behavior of phase-change medium. *Jpn. J. Appl. Phys.* **38,** 1649 (1999).
43. J. Park, M.R. Kim, W.S. Choi, H. Seo, and C. Yeon: Characterization of amorphous phases of $Ge_2Sb_2Te_5$ phase-change optical recording material on their crystallization behavior. *Jpn. J. Appl. Phys.* **38,** 4775 (1999).
44. H.E. Kissinger: Reaction kinetics in differential thermal analysis. *Anal. Chem.* **29,** 1702 (1957).
45. H. Iwasaki, M. Harigaya, O. Nonoyama, Y. Kageyama, M. Takahashi, K. Yamada, H. Deguchi, and Y. Ide: Completely erasable phase change optical disc II: Application of Ag–In–Sb–Te mixed-phase system for rewritable compact disc compatible with CD-velocity and double CD-velocity. *Jpn. J. Appl. Phys.* **32**(Pt. 1), 5241 (1993).